Submitted to

XXII International Symposium on Lepton-Photon Interactions at High Energy, June 30, 2005, Uppsala

Abstract: **386**

Session: **Electroweak physics and beyond**

www-h1.desy.de/h1/www/publications/conf/conf_list.html

Determination of Electroweak Parameters at HERA

H1 Collaboration

Abstract

Using the $e^{+}p$ and $e^{-}p$ charged and neutral current cross sections previously measured by the H1 experiment, a combined electroweak and QCD analysis is performed to determine electroweak parameters accounting for their correlation with parton distributions. An improved measurement is obtained of the W propagator mass in charged current ep scattering. The weak mixing angle $\sin^2\theta_W$ is determined in the on-mass-shell renormalisation scheme. A first measurement at HERA is made of the light quark weak couplings to the Z^0 boson.

1 Introduction

The deep inelastic scattering (DIS) of leptons off nucleons has played an important role in revealing the structure of matter, in the discovery of weak neutral current interactions and in the foundation of the Standard Model (SM) as the theory of strong and electroweak (EW) interactions. At HERA, the first lepton-proton collider ever built, the study of DIS has been pursued since 1992 over a wide kinematic range. In terms of Q^2, the negative four-momentum transfer squared, the kinematic coverage can extend up to the centre-of-mass energy squared (s), thus covering the region where the electromagnetic and weak interactions become of comparable strength. Both charged current (CC) and neutral current (NC) interactions occur in ep collisions and are studied by the two collider experiments H1 and ZEUS. The data taken in a first phase of the HERA operation (HERA-I) until 2000 have been used in many QCD analyses to determine the strong interaction coupling constant α_s [1, 2, 3] and parton distribution functions (PDFs) [2, 4, 5]. Based on the HERA-I data EW analyses have been also performed [4, 6, 7, 8, 9, 10, 11] to extract the W boson mass value from the CC data at high Q^2. Previously the QCD and EW sectors were analysed independently.

The increased precision of the H1 data recently published [1, 4, 8, 5] permits a combined QCD and EW analysis which is performed here for the first time. A measurement is made of the CC propagator mass (M_{prop}). The masses of the W boson (M_W) and top quark (m_t) and the weak mixing angle ($\sin^2\theta_W$) are determined within the electroweak $SU(2)_L \times U(1)$ Standard Model. The vector and axial-vector weak couplings of the light (u and d) quarks to the Z^0 boson are measured for the first time at HERA. These results are complementary to determinations of EW parameters at LEP, the Tevatron and low energy experiments [12].

2 Charged and Neutral Current Cross Sections

2.1 Charged Current Cross Section

The charged current interactions, $e^\pm p \to \overset{(-)}{\nu}_e X$, are mediated by the exchange of a W boson in the t channel. The measured cross section for unpolarised beams after correction for QED radiative effects [13] can be expressed as

$$\frac{d^2\sigma^{\text{CC}}(e^\pm p)}{dxdQ^2} = \frac{G_F^2}{2\pi x}\left[\frac{M_W^2}{M_W^2+Q^2}\right]^2 \phi^\pm_{CC}(x,Q^2)\left(1+\Delta^{\pm,weak}_{CC}\right), \tag{1}$$

$$\text{with} \quad \phi^\pm_{CC}(x,Q^2) = \frac{1}{2}\left[Y_+W_2^\pm(x,Q^2) \mp Y_- xW_3^\pm(x,Q^2) - y^2W_L^\pm(x,Q^2)\right]. \tag{2}$$

Here G_F is the Fermi constant accounting for radiative corrections to the W propagator as measured in muon decays and $\Delta^{\pm,weak}_{CC}$ represents the other weak vertex and box corrections, which amount to a few per mil [14] and are neglected. The term $\phi^\pm_{CC}$ [4] contains the structure functions $W_2^\pm$, $xW_3^\pm$ and $W_L^\pm$. The factors $Y_\pm$ are defined as $Y_\pm \equiv 1 \pm (1-y)^2$ and y is the inelasticity variable which is related to Bjorken x and Q^2 by $y = Q^2/xs$.

Within the SM, the CC cross section in Eqn.(1) can be expressed in the so-called on-mass-shell (OMS) scheme [15] by replacing the Fermi constant G_F by the following relation:

$$G_F = \frac{\pi\alpha}{\sqrt{2}M_W^2\left(1 - \frac{M_W^2}{M_Z^2}\right)} \frac{1}{1 - \Delta r}\,, \tag{3}$$

where $\alpha \equiv \alpha(Q^2 = 0)$ is the fine structure constant and M_Z is the mass of the Z^0 boson. The term Δr contains EW radiative corrections which can be expressed at one loop as [14]

$$\Delta r = \Delta\alpha - \frac{\cos^2\theta_W}{\sin^2\theta_W}\Delta\rho + \Delta r_{\rm rem}\,. \tag{4}$$

The first term $\Delta\alpha$ is the fermionic part of the photon vacuum polarisation. It has a calculable leptonic contribution and an uncalculable hadronic component which can however be estimated using e^+e^- data [16]. Numerically these two contributions are of similar size and have a total value of 0.059 [17] when evaluated at M_Z^2. The quantity $\Delta\rho$ arises from the large mass difference between the top and bottom quarks in the vector boson self-energy loop:

$$\Delta\rho = \frac{3\alpha}{16\pi\sin^2\theta_W\cos^2\theta_W}\frac{m_t^2}{M_Z^2}\,. \tag{5}$$

The second term in Eqn.(4) has a numerical value of about 0.03. The last term $\Delta r_{\rm rem}$ is numerically smaller (~ 0.01). It contains the remaining contributions including those with logarithmic dependence on m_t and the Higgs boson mass M_H. In Eqns.(4,5) and the OMS scheme, it is understood that

$$\sin^2\theta_W = 1 - M_W^2/M_Z^2 \quad \text{and} \quad \cos^2\theta_W = M_W^2/M_Z^2\,. \tag{6}$$

In the quark parton model (QPM), the structure functions $W_2^\pm$ and $xW_3^\pm$ may be interpreted as lepton charge dependent sums and differences of quark and anti-quark distributions and are given by

$$W_2^+ = x(\overline{U} + D),\quad xW_3^+ = x(D - \overline{U}),\quad W_2^- = x(U + \overline{D}),\quad xW_3^- = x(U - \overline{D})\,, \tag{7}$$

whereas $W_L^\pm = 0$. The terms xU, xD, $x\overline{U}$ and $x\overline{D}$ are defined as the sum of up-type, of down-type and of their anti-quark-type distributions, i.e., below the b quark mass threshold:

$$xU = x(u + c),\quad xD = x(d + s),\quad x\overline{U} = x(\overline{u} + \overline{c}),\quad x\overline{D} = x(\overline{d} + \overline{s})\,. \tag{8}$$

In next-to-leading-order (NLO) QCD and the $\overline{\rm MS}$ normalisation scheme [18], these simple relations do not hold any longer and $W_L^\pm$ becomes non-zero. Nevertheless the capability of the CC cross sections to probe up- and down-type quarks remains.

2.2 Neutral Current Cross Section

The NC interactions, $e^\pm p \to e^\pm X$, are mediated by photon (γ) or Z^0 exchange in the t channel. The measured NC cross section with unpolarised beams after correction for QED radiative effects [19] is given by

$$\frac{d^2\sigma^{\rm NC}(e^\pm p)}{dxdQ^2} = \frac{2\pi\alpha^2}{xQ^4}\phi_{NC}^\pm(x,Q^2)\left(1 + \Delta_{NC}^{\pm,weak}\right)\,, \tag{9}$$

$$\text{with}\quad \phi_{NC}^\pm(x,Q^2) = Y_+\tilde{F}_2(x,Q^2) \mp Y_- x\tilde{F}_3(x,Q^2) - y^2\tilde{F}_L(x,Q^2)\,. \tag{10}$$

Here $\Delta_{NC}^{\pm,weak}$ represents weak radiative corrections which are typically less than 1% and never more than 3%. The NC structure function term $\phi_{NC}^{\pm}$ [4] is expressed in terms of the generalised structure functions $\tilde{F}_2$, $x\tilde{F}_3$ and $\tilde{F}_L$. The first two can be further decomposed as [20]

$$\tilde{F}_2 \equiv F_2 - v_e \frac{\kappa Q^2}{(Q^2+M_Z^2)} F_2^{\gamma Z} + (v_e^2+a_e^2)\left(\frac{\kappa Q^2}{Q^2+M_Z^2}\right)^2 F_2^Z , \tag{11}$$

$$x\tilde{F}_3 \equiv - a_e \frac{\kappa Q^2}{(Q^2+M_Z^2)} xF_3^{\gamma Z} + (2v_e a_e)\left(\frac{\kappa Q^2}{Q^2+M_Z^2}\right)^2 xF_3^Z , \tag{12}$$

with

$$\kappa^{-1} = \frac{2\sqrt{2}\pi\alpha}{G_F M_Z^2} , \tag{13}$$

in the modified on-mass-shell (MOMS) scheme [21] in which all EW parameters can be defined in terms of α, G_F and M_Z (besides fermion masses and quark mixing angles) or

$$\kappa^{-1} = 4\frac{M_W^2}{M_Z^2}\left(1-\frac{M_W^2}{M_Z^2}\right)(1-\Delta r) \tag{14}$$

in the OMS scheme. The quantities v_e and a_e are the vector and axial-vector weak couplings of the electron to the Z^0 [12]. In the bulk of the HERA phase space, $\tilde{F}_2$ is dominated by the electromagnetic structure function F_2 originating from photon exchange only. The functions F_2^Z and xF_3^Z are the contributions to $\tilde{F}_2$ and $x\tilde{F}_3$ from Z^0 exchange and the functions $F_2^{\gamma Z}$ and $xF_3^{\gamma Z}$ are the contributions from γZ interference. These contributions only become important at large values of Q^2.

In the QPM, the longitudinal structure function $\tilde{F}_L = 0$, the structure functions F_2, $F_2^{\gamma Z}$ and F_2^Z are related to the sum of the quark and anti-quark momentum distributions, xq and $x\overline{q}$,

$$[F_2, F_2^{\gamma Z}, F_2^Z] = x\sum_q [e_q^2, 2e_q v_q, v_q^2+a_q^2]\{q+\overline{q}\} \tag{15}$$

and the structure functions $xF_3^{\gamma Z}$ and xF_3^Z to their difference,

$$[xF_3^{\gamma Z}, xF_3^Z] = 2x\sum_q [e_q a_q, v_q a_q]\{q-\overline{q}\} . \tag{16}$$

In Eqns.(15,16), e_q is the electric charge of quark q , and v_q and a_q are, respectively, the vector and axial-vector weak coupling constants of the quarks to the Z^0:

$$v_q = I_{q,L}^3 - 2e_q \sin^2\theta_W \tag{17}$$

$$a_q = I_{q,L}^3 \tag{18}$$

where $I_{q,L}^3$ is the third component of the weak isospin.

The weak radiative corrections $\Delta_{NC}^{\pm,weak}$ in Eqn.(9) correspond effectively to modifications of the weak neutral current couplings to so-called dressed couplings by four weak form factors ρ_{eq}, κ_e, κ_q and κ_{eq} [14]. The form factor ρ_{eq} has a numerical value very close to 1 for $Q^2 \lesssim 10\,000\,\mathrm{GeV}^2$ and only at very high Q^2 is a deviation of a few percent reached [14]. The form factors $\kappa_{e,q,eq}$ fall strongly with Q^2 [14] and approach 1 where the γZ and Z^0 contributions become significant. Given the current precision of the data used (Section 3), in the following analysis $\rho_{eq} = 1$ is assumed and the weak mixing angle in Eqn.(17) is replaced by an effective one $\sin^2\theta_W^{eff} = \kappa_q(1 - M_W^2/M_Z^2)$ where κ_q is assumed to be flavour independent.

3 Data Sets and Fit Strategies

The analysis performed here uses (as in [5]) the following H1 data sets: two low Q^2 data sets ($1.5 \leq Q^2 \leq 150\,\mathrm{GeV}^2$) [1], three high Q^2 NC data sets ($100 \leq Q^2 \leq 30\,000\,\mathrm{GeV}^2$) [4, 5, 8] and three high Q^2 CC data sets ($300 \leq Q^2 \leq 15\,000\,\mathrm{GeV}^2$) [4, 5, 8]. These data cover a Bjorken x range from $3 \cdot 10^{-5}$ to 0.65 depending on Q^2.

The low Q^2 data are dominated by systematic uncertainties which have a precision down to 2% in most of the covered region. The high Q^2 data on the other hand are mostly limited by the statistical precision which is up to 30% or larger for $Q^2 \gtrsim 10\,000\,\mathrm{GeV}^2$.

The combined EW-QCD analysis follows the same fit procedure used in [5]. The QCD analysis is performed using the DGLAP evolution equations [22] at NLO [23] in the $\overline{\mathrm{MS}}$ renormalisation scheme. All quarks are taken to be massless.

Fits are performed to the measured cross sections assuming the strong coupling constant to be equal to $\alpha_s(M_Z) = 0.1185$ [24]. The analysis uses an x-space program developed within the H1 Collaboration [25]. In the fit procedure, a χ^2 function which is defined in [1] is minimised. The minimisation takes into account correlations between data points caused by systematic uncertainties [5].

In the fits, five PDFs – gluon, xU, xD, $x\overline{U}$ and $x\overline{D}$ – are defined by 10 free parameters as in [5]. The PDFs obtained here are consistent with the H1 PDF 2000 [5]. For more details refer to [26]. Table 1 shows an overview of various fits that are performed in subsequent section to determine different EW parameters.

Fit	Scheme	Fixed parameters	
		CC	NC
G-M_{prop}-PDF	–	–	α, M_Z, M_W
M_{prop}-PDF	MOMS	G_F	α, G_F, M_Z
M_W-PDF	OMS	α, M_Z, m_t, M_H	
m_t-PDF	OMS	α, M_Z, M_W, M_H	
v_u-a_u-v_d-a_d-PDF	–	G_F, M_W	α, M_Z, M_W
v_u-a_u-PDF	–	G_F, M_W	$\alpha, M_Z, M_W, v_d, a_d$
v_d-a_d-PDF	–	G_F, M_W	$\alpha, M_Z, M_W, v_u, a_u$
$I^3_{u,R}$-$I^3_{d,R}$-PDF	–	G_F, M_W	$\alpha, M_Z, M_W, v_{q,L}, a_{q,L}$

Table 1: Summary of the fit assumptions. In the fits, in addition to the free parameters listed in the first column, the systematic correlation uncertainty parameters are allowed to vary (see Table 2 in [5]). The fixed parameters are set to values taken from [12] and M_H is set to $120\,\mathrm{GeV}$.

4 Results

4.1 Determination of Masses and $\sin^2\theta_W$

The CC cross section data allow a simultaneous determination of G_F and M_W and of the PDFs as independent parameters (fit G-$M_{\rm prop}$-PDF in Table 1). In this fit, the parameters G_F and M_W in Eqn.(1) are considered to be a normalisation variable G and a propagator mass $M_{\rm prop}$, respectively, independent of the SM. The sensitivity to G according to Eqn.(1) results from the normalisation of the CC cross section whereas the sensitivity to $M_{\rm prop}$ arises from the Q^2 dependence. The fit is performed including the NC cross section data in order to constrain the PDFs. The result of the fit to G and $M_{\rm prop}$ is shown in Fig. 1 as the shaded area. The χ^2 value per degree of freedom (dof) is $533.0/610 = 0.87$. The correlation between G, $M_{\rm prop}$ and the fitted PDF parameters may be found in [27]. The determination is consistent with the SM values demonstrating the universality of the CC interaction over a large range of Q^2 values.

Fixing G to G_F at the value of $1.16637 \cdot 10^{-5}\,{\rm GeV}^2$ obtained from the muon lifetime measurement [12], one may fit the CC propagator mass $M_{\rm prop}$ only. For this fit ($M_{\rm prop}$-PDF), the EW parameters are defined in the MOMS scheme and the propagator mass $M_{\rm prop}$ is considered to be independent of any other EW parameters. Note that in the MOMS scheme, the use of G_F makes the dependency of the CC and NC cross sections on m_t and M_H negligibly small.

The result of the fit, also shown in Fig. 1, is

$$M_{\rm prop} = 82.87 \pm 1.82_{\rm exp}\ {}^{+0.30}_{-0.16}\Big|_{\rm model}\ {\rm GeV}\,. \tag{19}$$

Here the first error is experimental and the second corresponds to uncertainties due to input parameters and model assumptions as introduced in Table 5 in [5] (e.g., the variation of $\alpha_s = 0.1185 \pm 0.0020$). The χ^2 value per dof is $533.3/611$ [26].

The propagator mass $M_{\rm prop}$ measured here in the space-like region can be compared with direct W boson mass measurements obtained in the time-like region by the Tevatron and LEP experiments [12]. The value is consistent with the world average of $M_W = 80.425 \pm 0.038$ GeV [12] within 1.3 standard deviations.

In comparison with previous measurements of $M_{\rm prop}$ at HERA [7, 4, 8, 9, 10, 11], the precision is improved. This is due to the higher statistics data and the different treatment of the correlation between the propagator mass and the PDFs.

Within the SM, the CC and NC cross sections can be expressed in the OMS scheme in which all EW parameters are determined by α, M_Z and M_W together with m_t and M_H in the loop corrections. In this scheme, the CC cross section normalisation depends on M_W via the $G_F - M_W$ relation (Eqn.(3)). Some additional sensitivity to M_W comes through the M_W dependent terms (e.g., Eqn.(14)) in the NC cross section. Fixing m_t to its world average value of 178 GeV [12] and assuming $M_H = 120$ GeV, the fit M_W-PDF leads to

$$M_W = 80.786 \pm 0.205_{\rm exp}\ {}^{+0.048}_{-0.029}\Big|_{\rm model} \pm 0.025_{\delta m_t} - 0.084_{\delta M_H} \pm 0.033_{\delta(\Delta r)}\ {\rm GeV}\,. \tag{20}$$

Here, in addition to the experimental and model uncertainties, three other error sources are considered: the uncertainty on the top quark mass $\delta m_t = 4.3$ GeV [12], a variation of the Higgs mass from $120\,\mathrm{GeV}$ to $300\,\mathrm{GeV}$ and the uncertainty of higher order terms in Δr [26]. It should be pointed out that the result (20) on M_W is not a direct measurement but a determination within the SM framework.

Together with the world average value of $M_Z = 91.1876 \pm 0.0021\,\mathrm{GeV}$ [12], the result obtained on M_W from Eqn.(20) represents an indirect determination of $\sin^2\theta_W$ in the OMS scheme (Eqn.(6))

$$\sin^2\theta_W = 0.2151 \pm 0.0040_{\mathrm{exp}} \,{}^{+0.0019}_{-0.0011}\Big|_{\mathrm{th}} \tag{21}$$

where the first error is experimental and the second is theoretical covering all remaining uncertainties in Eqn.(20). The uncertainty due to δM_Z is negligible.

Figure 2 shows the correlation between M_W and m_t in a simultaneous fit to these parameters. Fixing M_W to the world average value and assuming $M_H = 120\,\mathrm{GeV}$, the fit m_t-PDF gives $m_t = 108 \pm 44\,\mathrm{GeV}$ where the uncertainty is experimental. The result represents the first determination of the top quark mass through loop effects in the ep data at HERA.

4.2 Determination of $v_{u,d}$ and $a_{u,d}$

At HERA, the NC interactions at high Q^2 receive contributions from γZ interference and Z^0 exchange (Eqns.(15,16)). Thus the NC data can be used to extract the weak couplings of up- and down-type quarks to the Z^0 boson. At high Q^2 and high x, where the NC $e^{\pm}p$ cross sections are sensitive to these couplings, the up- and down-type quark distributions are dominated by the light u and d quarks. Therefore, this measurement can be considered to determine the light quark couplings. The CC cross section data help disentangle the up and down quark distributions.

In this analysis (fit v_u-a_u-v_d-a_d-PDF), the vector and axial-vector dressed couplings of u and d quarks are treated as free parameters. The results of the fit are shown in Fig. 3 and are given in Table 2. The effect of the u and d correlation is illustrated in Fig. 3 by fixing either u or d quark couplings to their SM values (fits v_d-a_d-PDF and v_u-a_u-PDF). The precision is better for the u quark as expected. The superior precision for a_u comes from the γZ interference contribution $xF_3^{\gamma Z}$ (Eqn.(16)). The d-quark couplings v_d and a_d are mainly constrained by the Z^0 exchange term F_2^Z (Eqn.(15)). These differences in sensitivity result in different contour shapes shown in Fig. 3.

Fit	a_u	v_u	a_d	v_d	χ^2/dof
v_u-a_u-v_d-a_d-PDF	0.56 ± 0.10	0.05 ± 0.19	-0.77 ± 0.37	-0.50 ± 0.37	$531.7/608$
v_u-a_u-PDF	0.57 ± 0.08	0.27 ± 0.13	–	–	$534.1/610$
v_d-a_d-PDF	–	–	-0.80 ± 0.24	-0.33 ± 0.33	$532.6/610$
SM value	0.5	0.196	-0.5	-0.346	–

Table 2: The results of the fits to the weak neutral current couplings in comparison with their SM values. The correlation between the the fit parameters may be found in [28].

The results from this analysis are also compared in Fig. 3 with the combined LEP data where all possible solutions are explicitly shown [29]. The HERA determination is sensitive to u and

d quarks separately, contrary to other precise measurement of light quark-Z^0 couplings in νN scattering [30] and atomic partity violation [31] on heavy nuclei. The HERA determination also resolves the ambiguities present in the LEP results.

5 Conclusion

Using the neutral and charged current cross section data recently published by H1, combined electroweak and QCD fits have been performed. This analysis is the first in which the correlation between the electroweak and parton distribution parameters is considered and a set of electroweak theory parameters is determined in the space-like region based on the HERA data.

Exploiting the Q^2 dependence of the charged current data, the propagator mass has been measured with the result $M_{\rm prop} = 82.87 \pm 1.82_{\rm exp}\ {}^{+0.30}_{-0.16}\big|_{\rm model}$. Within the Standard Model framework, the W mass has been determined to be $M_W = 80.786 \pm 0.205_{\rm exp}\ {}^{+0.063}_{-0.098}\big|_{\rm th}$ GeV in the on-mass-shell scheme. This mass value has also been used to derive an indirect determination of $\sin^2\theta_W$ yielding $0.2151 \pm 0.0040_{\rm exp}\ {}^{+0.0019}_{-0.0011}\big|_{\rm th}$. Furthermore, a result on the top quark mass via electroweak effects in ep data has been obtained.

The vector and axial-vector weak neutral current couplings of u and d quarks to the Z^0 boson have been determined at HERA for the first time.

Acknowledgements

We are grateful to the HERA machine group whose outstanding efforts have made this experiment possible. We thank the engineers and technicians for their work in constructing and maintaining the H1 detector, our funding agencies for financial support, the DESY technical staff for continual assistance and the DESY directorate for support and for the hospitality which they extend to the non DESY members of the collaboration. It is our pleasure to thank H. Spiesberger for helpful discussions.

References

[1] C. Adloff *et al.* [H1 Collaboration], Eur. Phys. J. **C21** (2001) 33 [hep-ex/0012053].

[2] S. Chekanov *et al.* [ZEUS Collaboration], Phys. Rev. **D67** (2003) 012007 [hep-ex/0208023].

[3] S. Chekanov *et al.* [ZEUS Collaboration], submitted to Eur. Phys. J. [hep-ph/0503274].

[4] C. Adloff *et al.* [H1 Collaboration], Eur. Phys. J. **C13** (2000) 609 [hep-ex/9908059].

[5] C. Adloff *et al.* [H1 Collaboration], Eur. Phys. J. **C30** (2003) 1 [hep-ex/0304003].

[6] T. Ahmed *et al.* [H1 Collaboration], Phys. Lett. B **324** (1994) 241.

[7] S. Aid *et al.* [H1 Collaboration], Phys. Lett. B **379** (1996) 319 [hep-ex/9603009].

[8] C. Adloff *et al.* [H1 Collaboration], Eur. Phys. J. **C19** (2001) 269 [hep-ex/0012052].

[9] J. Breitweg *et al.* [ZEUS Collaboration], Eur. Phys. J. **C12** (2000) 411 [hep-ex/9907010]; [Erratum ibid. **B27** (2003) 305].

[10] S. Chekanov *et al.* [ZEUS Collaboration], Phys. Lett. **B539** (2002) 197 [hep-ex/0205091]; [Erratum ibid. B **552** (2003) 308].

[11] S. Chekanov *et al.* [ZEUS Collaboration], Eur. Phys. J. **C32** (2003) 1 [hep-ex/0307043].

[12] S. Eidelman *et al.* [Particle Data Group Collaboration], Phys. Lett. **B592** (2004) 1.

[13] D. Y. Bardin, K. C. Burdik, P. K. Khristova and T. Riemann, Z. Phys. C **44** (1989) 149; M. Böhm and H. Spiesberger, Nucl. Phys. B **304** (1988) 749; H. Spiesberger, Nucl. Phys. B **349** (1991) 109.

[14] W. Hollik *et al.*, Proceedings of the Workshop "Physics at HERA", vol.2, eds. W. Buchmüller and G. Ingelman, DESY (1992) 923.

[15] A. Sirlin, Phys. Rev. **D22** (1980) 971 and ibid. **D29** (1984) 89.

[16] See e.g., M. Davier, S. Eidelman, A. Höcker and Z. Zhang, Eur. Phys. J. **C27**, 497 (2003) [hep-ph/0208177] and references therein.

[17] H. Spiesberger, http://www.desy.de/∼hspiesb/eprc.html.

[18] W. A. Bardeen, A. J. Buras, D. W. Duke and T. Muta, Phys. Rev. D **18** (1978) 3998.

[19] H. Spiesberger *et al.*, Proceedings of the Workshop "Physics at HERA", vol.2, eds. W. Buchmüller and G. Ingelman, DESY (1992) 798.

[20] M. Klein and T. Riemann, Z. Phys. **C24** (1984) 151.

[21] W. F. L. Hollik, Fortschr. Phys. **38** (1990) 165.

[22] Y. L. Dokshitzer, Sov. Phys. JETP **46** (1977) 641 [Zh. Eksp. Teor. Fiz. **73** (1977) 1216]; V. N. Gribov and L. N. Lipatov, Yad. Fiz. **15** (1972) 1218 [Sov. J. Nucl. Phys. **15** (1972) 675]; V. N. Gribov and L. N. Lipatov, Yad. Fiz. **15** (1972) 781 [Sov. J. Nucl. Phys. **15** (1972) 438]; G. Altarelli and G. Parisi, Nucl. Phys. **B126** (1977) 298.

[23] W. Furmanski and R. Petronzio, Phys. Lett. **B97** (1980) 437.

[24] D. E. Groom *et al.* [Particle Data Group Collaboration], Eur. Phys. J. **C15** (2000) 1.

[25] C. Pascaud and F. Zomer, LAL preprint, LAL 95-05 (1995);
C. Pascaud and F. Zomer, hep-ph/0104013.

[26] B. Portheault, Ph.D. thesis, LAL preprint, LAL 05-05 (March 2005), IN2P3-CNRS et Université de Paris-Sud.

[27] See http://www-h1.desy.de/psfiles/figures/d05-xxx.gf-mw.correlation for the uncertainties on the parameters and their correlations.

[28] See http://www-h1.desy.de/psfiles/figures/d05-xxx.vq-aq.correlation for the uncertainties on the parameters and their correlations.

[29] LEP EW working group, http://lepewwg.web.cern.ch/LEPEWWG/plots/summer2004/.

[30] G. P. Zeller *et al.* [NuTeV Collaboration], Phys. Rev. Lett. **88** (2002) 091802 [Erratum-ibid. **90** (2003) 239902] [hep-ex/0110059].

[31] S. C. Bennett and C. E. Wieman, Phys. Rev. Lett. **82** (1999) 2484 [hep-ex/9903022].

[32] See e.g., M. Klein, T. Riemann and I. A. Savin, Phys. Lett. **B85** (1979) 385.

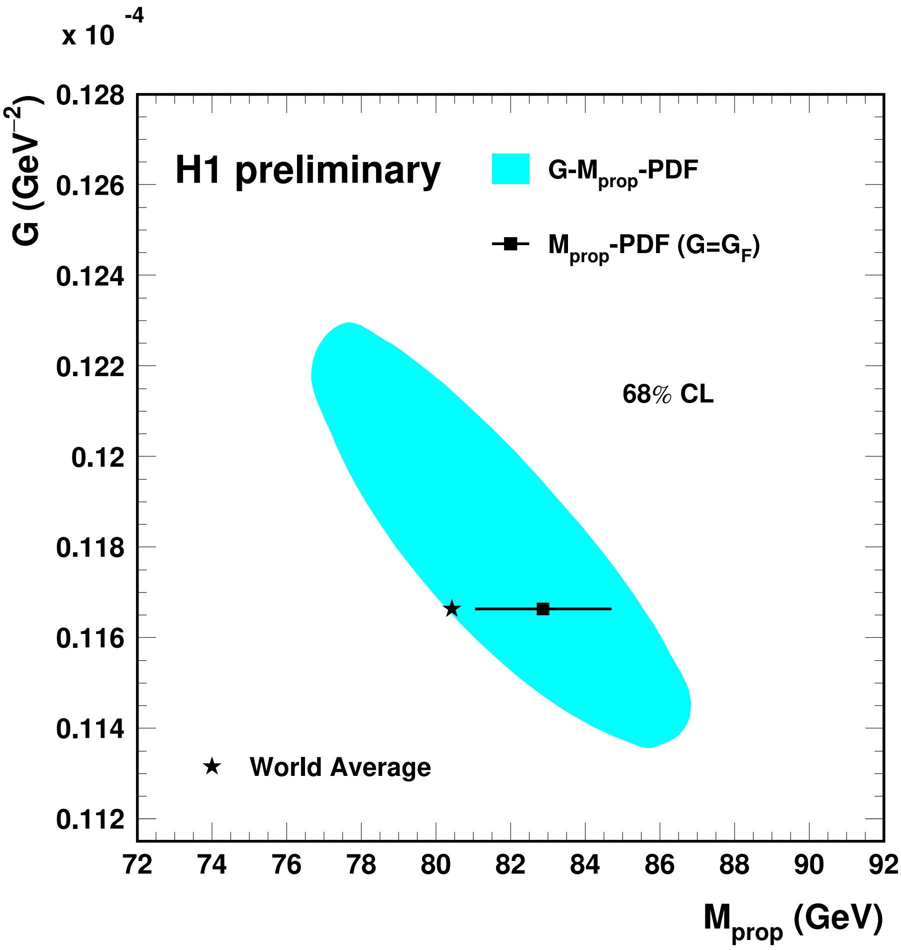

Figure 1: The result of the fit to G and M_{prop} at 68% confidence level (CL) shown as the shaded area. The world average values are indicated with the star symbol. Fixing G to G_F, the fit in the MOMS scheme results in a measurement of the propagator mass M_{prop} shown as the square with the horizontal error bars.

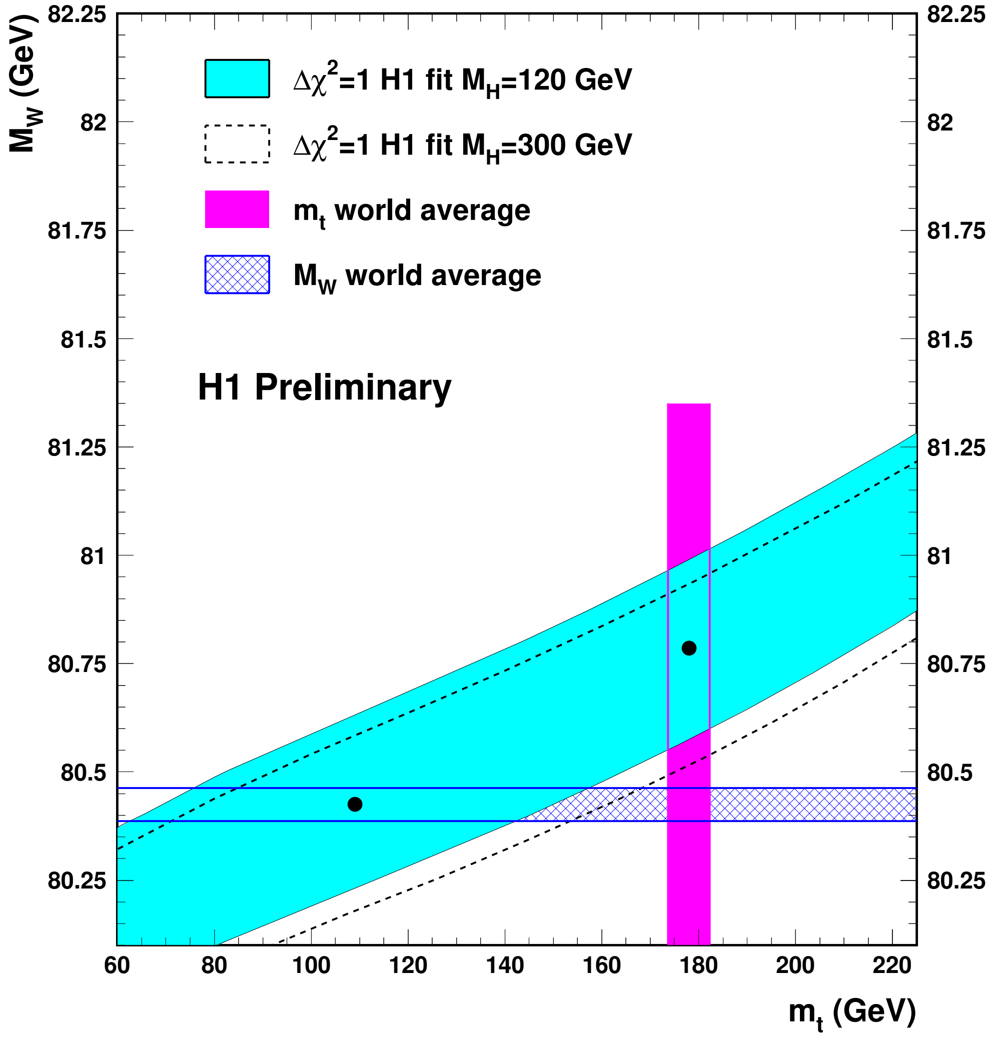

Figure 2: The fitted M_W as a function of m_t shown for $M_H = 120\,\mathrm{GeV}$ (the large shaded band) and $M_H = 300\,\mathrm{GeV}$ (the area between the two dashed lines). The vertical shaded band and the horizontal hatched band show the world average values of m_t and M_W respectively.

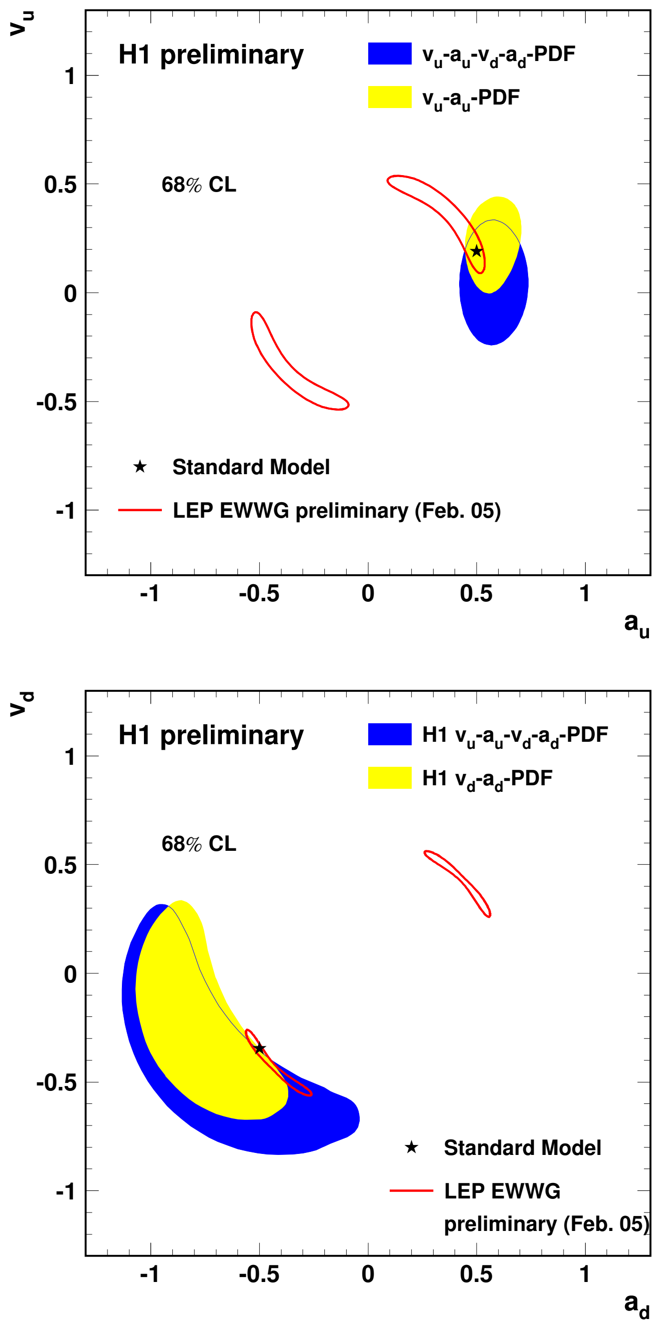

Figure 3: Results at 68% confidence level (CL) on the weak neutral current couplings of u (upper plot) and d (lower plot) quarks to the Z^0 boson determined in this analysis (the shaded contours) in comparison with those determined by the combined LEP data which have both sign and $v - a$ exchange ambiguities. The dark-shaded contours correspond to results of a simultaneous fit of all four couplings whereas the lighted-shaded contours correspond to results of fits where either d or u quark couplings are fixed to their SM values. The stars show the expected SM values.